PATH TRACKING CONTROL OF TRACTORS AND STEERABLE IMPLEMENTS BASED ON KINEMATIC AND DYNAMIC MODELING

R. Werner, S. Mueller

Institute of Mechatronics in Mechanical and Automotive Engineering
University of Kaiserslautern
Kaiserslautern, Germany

G. Kormann

John Deere European Technology Innovation Center
Deere & Company
Kaiserslautern, Germany

ABSTRACT

Precise path tracking control of tractors and implements is a key factor for automation of agriculture. Path tracking controllers for tractors are highly developed and the focus is now on precise control of implements. Most recently the attention was drawn to implements being equipped with steering actuators themselves. For control of those steerable implements understanding the underlying vehicle dynamics now becomes essential. This work therefore derives easily extensible kinematic and dynamic models for tractors and steerable towed implements. A flexible path tracking controller allowing to combine steering options freely is presented for the overall system. Finally a system analysis is performed and simulation results comparing kinematic and dynamic model based control approaches are presented in order to facilitate choosing the appropriate model.

Keywords: steerable implement, kinematic and dynamic model, path tracking

INTRODUCTION

Path tracking control of tractors became the enabling technology for automation of field work in recent years. More and more sophisticated tractor control systems however revealed that exact positioning of the actual implement is equally or even more important. Especially sloped and curved terrain, strip till fields and buried drip irrigation tapes require precise implement control. For this reason the attention is now drawn to path tracking control using actively steered implements. Despite the existence of first path tracking control systems for steerable implements, little is known about the underlying kinematic and dynamic properties of tractor and steerable implement combinations. As a consequence design and setup of those path tracking control systems mainly depend on in-field adjustments performed first by the developer and later by the operator. Understanding the underlying kinematic and dynamic principles now becomes essential for further development of those systems.

Kinematic models, i.e. models disregarding forces associated with tractor and implement motion, of unsteered implements are subject to research by (Bell, 1999), (Bevly, 2001) and (Cariou et al., 2010). (Backman, 2009) presented a kinematic model with steerable drawbar.

Dynamic modeling of on-road truck and unsteered trailer combinations has been around for a long time and the systematic approaches presented by (Genta, 1997) and (Chen and Tomizuka, 1995) proved to be useful for this work. Off-road tractor and unsteered implement dynamics are subject to research by (Karkee and Steward, 2010). (Pota et al., 2007) and (Siew et al., 2009) with little additional effort added steerable wheels to a dynamic implement model. This is in contrast to the large effort necessary for dynamic modeling of steering actuators between tractor and implement, e.g. a steerable drawbar. The time dependent constraints introduced with those actuators turn out to result in very lengthy expressions.

In order to handle those expressions this work uses a very systematic approach based on Lagrangian mechanics originally proposed for unsteered truck trailer combinations (Genta, 1997). This approach has been extended to steered implements and was presented previously in (Werner et al., 2012). In addition now a systematic approach for kinematic modeling of tractors and steerable implements is included, with both approaches suitable for simple addition or replacement of actuators. Considering both the kinematic and the dynamic model allows for direct comparison and supports choosing the appropriate model for the given task. Due to simple parameterization, of course, a kinematic model is preferred for model based controller design, as long as it is able to provide a suitable description of the actual system. System analysis is performed with both models and linearized versions of both models are used for path tracking controller design. Several path tracking controllers for the resulting multiple-input and multiple output (MIMO) system are proposed. Finally simulation results are presented comparing performance of controllers based on either kinematic or dynamic model descriptions.

TRACTOR AND STEERABLE IMPLEMENT MODEL

With focus on path tracking and lateral dynamics a bicycle model approach is chosen for both kinematic and dynamic modeling. Fig. 1 depicts the bicycle model of a front-steering tractor towing an implement with steerable wheels and steerable drawbar. The bicycle model is limited to plane motion. Roll and pitch movement as well as wheel load transfer are neglected, yet the influence of gravity on slopes will be considered by introducing disturbances. For later use the x-y-coordinate transformation matrices $\mathbf{T}_{t,e}$, $\mathbf{T}_{r1d,e}$, and $\mathbf{T}_{r1,e}$ from tractor-fixed, drawbar-fixed, and implement-fixed to earth-fixed coordinates can be found to be:

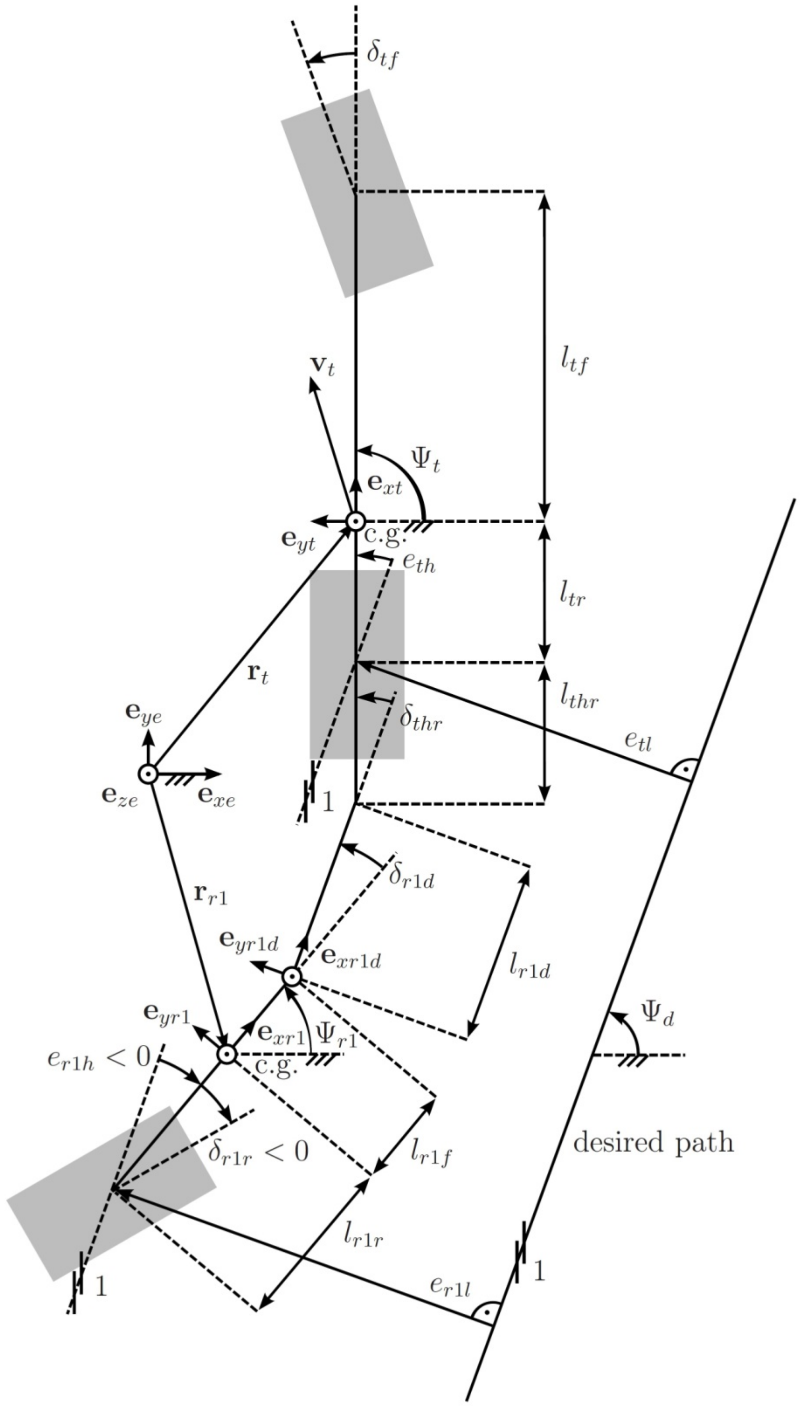

Fig. 1. Tractor and steerable implement bicycle model with earth-fixed ($\mathbf{e}_{xe}$, $\mathbf{e}_{ye}$, $\mathbf{e}_{ze}$), tractor-fixed ($\mathbf{e}_{xt}$, $\mathbf{e}_{yt}$, $\mathbf{e}_{zt}$), implement-fixed ($\mathbf{e}_{xr1}$, $\mathbf{e}_{yr1}$, $\mathbf{e}_{zr1}$), drawbar-fixed ($\mathbf{e}_{xr1d}$, $\mathbf{e}_{yr1d}$, $\mathbf{e}_{zr1d}$) coordinate systems, tractor wheel steering angle δ_{tf}, implement wheel steering angle δ_{r1r}, drawbar steering angle δ_{r1d}, hitch angle δ_{thr}, tractor heading angle Ψ_t, implement heading angle Ψ_{r1}, orientation of the desired path Ψ_d, tractor lateral error e_{tl}, tractor heading error e_{th}, implement lateral error e_{r1l} , implement heading error e_{r1h}, and all geometric parameters required.

$$\left.\begin{aligned}\mathbf{T}_{t,e} &= \mathbf{T}(\Psi_t)\\ \mathbf{T}_{r1d,e} &= \mathbf{T}(\Psi_t-\delta_{thr})\\ \mathbf{T}_{r1,e} &= \mathbf{T}(\Psi_t-\delta_{thr}-\delta_{r1d})\end{aligned}\right\}\text{with } \mathbf{T}(\bullet)=\begin{bmatrix}\cos(\bullet) & -\sin(\bullet)\\ \sin(\bullet) & \cos(\bullet)\end{bmatrix}. \qquad [1]$$

Kinematic Equations of Motion

Kinematic vehicle models provide a simplified description of the actual vehicle movement. Instead of deriving the equations of motion on foundations of dynamic principles taking into account forces and moments, those equations are derived from more idealized constraints. First of all the tractor longitudinal velocity v_t^{xt} is assumed to be an input to the system, disregarding what actually causes that velocity. In addition the vehicle's velocity vectors at the wheels in Fig. 1 are assumed to be aligned with the according wheel's longitudinal direction, i.e. no wheel side-slip occurs. Defining the vectors $\mathbf{e}_{tf}$ and $\mathbf{e}_{r1r}$ perpendicular to the longitudinal axis of tractor front and implement wheel respectively and using the velocities $\mathbf{v}_{tf}$ and $\mathbf{v}_{r1r}$ at tractor front and implement wheel those constraints are given by

$$\mathbf{e}_{tf}^{\mathrm{T}}\mathbf{v}_{tf}=0, \qquad [2]$$

$$\mathbf{e}_{r1r}^{\mathrm{T}}\mathbf{v}_{r1r}=0, \qquad [3]$$

or using tractor-fixed coordinates

$$\begin{bmatrix}-\sin(\delta_{tf}) & \cos(\delta_{tf})\end{bmatrix}\begin{bmatrix}v_{tf}^{xt}\\ v_{tf}^{yt}\end{bmatrix}=0, \qquad [4]$$

$$\begin{bmatrix}-\sin(\delta_{r1r}-\delta_{r1d}-\delta_{thr}) & \cos(\delta_{r1r}-\delta_{r1d}-\delta_{thr})\end{bmatrix}\begin{bmatrix}v_{r1r}^{xt}\\ v_{r1r}^{yt}\end{bmatrix}=0. \qquad [5]$$

In order to obtain the unknown velocities in Eq. [4] and [5] tractor front wheel position $\mathbf{r}_{tf}$ and implement wheel position $\mathbf{r}_{r1r}$ are related to the tractor rear wheel position $\mathbf{r}_{tr}$ using earth-fixed coordinates and Eq. [1]:

$$\begin{bmatrix}r_{tf}^{xe}\\ r_{tf}^{ye}\end{bmatrix}=\begin{bmatrix}r_{tr}^{xe}\\ r_{tr}^{ye}\end{bmatrix}+\mathbf{T}_{t,e}\begin{bmatrix}l_{tr}+l_{tf}\\ 0\end{bmatrix}, \qquad [6]$$

$$\begin{bmatrix}r_{r1r}^{xe}\\ r_{r1r}^{ye}\end{bmatrix}=\begin{bmatrix}r_{tr}^{xe}\\ r_{tr}^{ye}\end{bmatrix}+\mathbf{T}_{t,e}\begin{bmatrix}-l_{thr}\\ 0\end{bmatrix}+\mathbf{T}_{r1d,e}\begin{bmatrix}-l_{r1d}\\ 0\end{bmatrix}+\mathbf{T}_{r1,e}\begin{bmatrix}-l_{r1f}-l_{r1r}\\ 0\end{bmatrix}. \qquad [7]$$

Calculating the time derivatives of Eq. [6] and [7], substituting

$$\frac{d}{dt}\begin{bmatrix}r_{tr}^{xe}\\ r_{tr}^{ye}\end{bmatrix}=\mathbf{T}_{t,e}\begin{bmatrix}v_t^{xt}\\ 0\end{bmatrix}, \qquad [8]$$

and transforming the result into tractor-fixed coordinates yields

$$\begin{bmatrix}v_{tf}^{xt}\\ v_{tf}^{yt}\end{bmatrix}=\begin{bmatrix}v_t^{xt}\\ \dot{\Psi}_t\left(l_{tr}+l_{tf}\right)\end{bmatrix} \qquad [9]$$

and a lengthy expression for $\begin{bmatrix}v_{r1r}^{xt} & v_{r1r}^{yt}\end{bmatrix}^{\mathrm{T}}$ omitted here. Using both expressions it is possible to solve Eq. [4] and [5] for $\dot{\Psi}_t$ and $\dot{\delta}_{thr}$ finally resulting in:

$$\dot{\Psi}_t = \frac{v_t^{xt}}{\left(l_{tr} + l_{tf}\right)} \tan\left(\delta_{tf}\right), \quad [10]$$

$$\dot{\delta}_{thr} = num/den \quad [11]$$

with

$$\begin{aligned} num = \{ & \left[\sin\left(\delta_{tf} + \delta_{thr} + \delta_{r1d} - \delta_{r1r}\right) \right. \\ & \left. - \sin\left(-\delta_{tf} + \delta_{thr} + \delta_{r1d} - \delta_{r1r}\right)\right] l_{thr} \\ & + \left[\sin\left(\delta_{tf} - \delta_{thr} - \delta_{r1d} + \delta_{r1r}\right) \right. \\ & \left. - \sin\left(\delta_{tf} + \delta_{thr} + \delta_{r1d} - \delta_{r1r}\right)\right] \left(l_{tr} + l_{tf}\right) \\ & + \left[\sin\left(\delta_{tf} + \delta_{r1d} - \delta_{r1r}\right) \right. \\ & \left. - \sin\left(-\delta_{tf} + \delta_{r1d} - \delta_{r1r}\right)\right] l_{r1d} \\ & + \left[\sin\left(\delta_{tf} + \delta_{r1r}\right) - \sin\left(-\delta_{tf} + \delta_{r1r}\right)\right] \left(l_{r1r} \right. \\ & \left. + l_{r1f}\right)\} \, v_t^{xt} \\ & - \left[\cos\left(-\delta_{tf} + \delta_{r1r}\right) + \cos\left(\delta_{tf} + \delta_{r1r}\right)\right] \left(l_{r1r} + l_{r1f}\right) \left(l_{tr} \right. \\ & \left. + l_{tf}\right) \dot{\delta}_{r1d}, \end{aligned} \quad [12]$$

$$\begin{aligned} den = \left(l_{tr} + l_{tf}\right)\{ & \left[\cos\left(-\delta_{tf} + \delta_{r1d} - \delta_{r1r}\right) \right. \\ & \left. + \cos\left(\delta_{tf} + \delta_{r1d} - \delta_{r1r}\right)\right] l_{r1d} \\ & + \left[\cos\left(-\delta_{tf} + \delta_{r1r}\right) + \cos\left(\delta_{tf} + \delta_{r1r}\right)\right]\left(l_{r1r} + l_{r1f}\right)\}. \end{aligned} \quad [13]$$

Note that with Eq. [12] the first order derivative of the drawbar steering angle $\dot{\delta}_{r1d}$ is assumed to exist. Within this work this is ensured by adding steering actuator dynamics including underlying steering angle control.

Dynamic Equations of Motion

Rigid body dynamics

In addition to the simple kinematic equations of motion Eq. [10–13] based on rather ideal assumptions and mostly geometric properties, now a dynamic description of tractor and steerable implement motion is derived. The according equations of motion are based on dynamic principles accounting for forces and moments causing the vehicle movement. Tractor and implement are now considered rigid bodies with masses m_t and m_{r1} and moments of inertia I_t and I_{r1} about $\mathbf{e}_{zt}$ and $\mathbf{e}_{zr1}$ at the respective center of gravity (c.g.). Using the transformation matrices Eq. [1] the constraints relating tractor and implement c.g. positions $\mathbf{r}_t$ and $\mathbf{r}_{r1}$ in earth-fixed coordinates are:

$$\begin{bmatrix} r_{r1}^{xe} \\ r_{r1}^{ye} \end{bmatrix} = \begin{bmatrix} r_t^{xe} \\ r_t^{ye} \end{bmatrix} + \mathbf{T}_{t,e} \begin{bmatrix} -l_{tr} - l_{thr} \\ 0 \end{bmatrix} + \mathbf{T}_{r1d,e} \begin{bmatrix} -l_{r1d} \\ 0 \end{bmatrix} + \mathbf{T}_{r1,e} \begin{bmatrix} -l_{r1f} \\ 0 \end{bmatrix}. \quad [14]$$

With the externally enforced drawbar steering angle δ_{r1d} in transformation matrix $\mathbf{T}_{r1,e}$ those constraints turn out to be explicitly time dependent. This results in very lengthy expressions making a manual derivation of the dynamic equations of motion unfeasible. To overcome this difficulty those equations are derived using an automated systematic procedure and computer algebra software. Lagrangian mechanics as well as thoughtful choice of generalized coordinates and transformations are key to this automated procedure. The approach sketched in this paper was presented previously (Werner et al., 2012) and extends the original method for trucks and unsteered trailers by (Genta, 1997). The latter also states a concise example for a smaller system.

Here the generalized coordinates $q_i, i = 1 \dots 4$ for the remaining degrees of freedom are chosen to be

$$q_1 = r_t^{xe}, \qquad q_2 = r_t^{ye}, \qquad q_3 = \Psi_t, \qquad q_4 = \delta_{thr}. \qquad [15]$$

With Eq. [14] this results in the transformations from generalized to earth-fixed coordinates:

$$\begin{bmatrix} r_t^{xe} \\ r_t^{ye} \end{bmatrix} = \begin{bmatrix} q_1 \\ q_2 \end{bmatrix}, \qquad [16]$$

$$\Psi_t = q_3, \qquad [17]$$

$$\begin{bmatrix} r_{r1}^{xe} \\ r_{r1}^{ye} \end{bmatrix} = \begin{bmatrix} q_1 - (l_{tr} + l_{thr})\cos(\mathrm{q}_3) - \mathrm{l}_{\mathrm{r1d}}\cos(\mathrm{q}_3 - \mathrm{q}_4) - \mathrm{l}_{\mathrm{r1f}}\cos(\mathrm{q}_3 - \mathrm{q}_4 - \delta_{r1d}) \\ q_2 - (l_{tr} + l_{thr})\sin(\mathrm{q}_3) - \mathrm{l}_{\mathrm{r1d}}\sin(\mathrm{q}_3 - \mathrm{q}_4) - \mathrm{l}_{\mathrm{r1f}}\sin(\mathrm{q}_3 - \mathrm{q}_4 - \delta_{r1d}) \end{bmatrix} \qquad [18]$$

$$\Psi_{r1} = q_3 - q_4 - \delta_{r1d}. \qquad [19]$$

The kinetic energy T (Greenwood, 1988) of tractor and implement is

$$T = \frac{1}{2} m_t \|\mathbf{v}_t\|^2 + \frac{1}{2} m_{r1} \|\mathbf{v}_{r1}\|^2 + \frac{1}{2} I_t (\omega_t^{ze})^2 + \frac{1}{2} I_{r1} (\omega_{r1}^{ze})^2 \qquad [20]$$

with

$$\mathbf{v}_t = \dot{\mathbf{r}}_t = \begin{bmatrix} \dot{r}_t^{xe} \\ \dot{r}_t^{ye} \end{bmatrix}, \ \mathbf{v}_{r1} = \dot{\mathbf{r}}_{r1} = \begin{bmatrix} \dot{r}_{r1}^{xe} \\ \dot{r}_{r1}^{ye} \end{bmatrix}, \ \omega_t^{ze} = \dot{\Psi}_t, \ \omega_{r1}^{ze} = \dot{\Psi}_{r1}. \qquad [21]$$

Combining Eq. [16–21] results in the kinetic energy T being a function of generalized coordinates $q_i, i = 1 \dots 4$ and drawbar steering angle δ_{r1d} as well as their first order time derivatives.

Without a potential energy function V modeling conservative forces Lagrange's equations of motion are:

$$\frac{d}{dt}\left(\frac{\partial T}{\partial \dot{q}_i}\right) - \frac{\partial T}{\partial q_i} = Q_i, \text{with } i = 1 \dots 4. \qquad [22]$$

The generalized forces Q_i of Eq. [22] are yet to be determined. Their purpose in this paper is to account for wheel forces and disturbing forces resulting from gravity. For a more general result however generalized forces are calculated assuming arbitrary external forces F_t^{xe}, F_t^{ye}, F_{r1}^{xe}, F_{r1}^{ye} acting on tractor and implement c.g. as well as moments M_t^{ze}, M_{r1}^{ze} about $\mathbf{e}_{zt}$ and $\mathbf{e}_{zr1}$.

The generalized forces Q_i are then given by (Greenwood, 1988)

$$Q_i = F_t^{xe}\gamma_{t,i}^{xe} + F_t^{ye}\gamma_{t,i}^{ye} + M_t^{ze}\beta_{t,i}^{ze} + F_{r1}^{xe}\gamma_{r1,i}^{xe} + F_{r1}^{ye}\gamma_{r1,i}^{ye} + M_{r1}^{ze}\beta_{r1,i}^{ze}, \qquad [23]$$

with the velocity and angular velocity coefficients

$$\boldsymbol{\gamma}_{t,i} = \frac{\partial \dot{\mathbf{r}}_t}{\partial \dot{q}_i} = \frac{\partial \mathbf{r}_t}{\partial q_i},\ \beta_{t,i}^{ze} = \frac{\partial \omega_t^{ze}}{\partial \dot{q}_i},\ \boldsymbol{\gamma}_{r1,i} = \frac{\partial \dot{\mathbf{r}}_{r1}}{\partial \dot{q}_i} = \frac{\partial \mathbf{r}_{r1}}{\partial q_i},\ \beta_{r1,i}^{ze} = \frac{\partial \omega_{r1}^{ze}}{\partial \dot{q}_i}. \quad [24]$$

The equations of motion given by Eq. [22–24] and subsequent substitutions using Eq. [15] yield equations with accelerations, velocities, forces, etc. in earth-fixed coordinates. This allows for numerical integration. Linearization required for controller design however is not possible because $q_3 = \Psi_t$ in general is not a small angle. To overcome that problem equations of motion in vehicle-fixed coordinates have to be found. This is done by first calculating only the partial derivatives in Eq. [22] and [24]. In a next step generalized coordinates are replaced by earth-fixed coordinates using Eq. [15]. Subsequently with Eq. [1] forces and moments, are stated in tractor and implement-fixed coordinates using

$$\begin{bmatrix} F_t^{xe} \\ F_t^{ye} \end{bmatrix} = \mathbf{T}_{t,e} \begin{bmatrix} F_t^{xt} \\ F_t^{yt} \end{bmatrix},\ M_t^{ze} = M_t^{zt}, \begin{bmatrix} F_{r1}^{xe} \\ F_{r1}^{ye} \end{bmatrix} = \mathbf{T}_{r1,e} \begin{bmatrix} F_{r1}^{xr1} \\ F_{r1}^{yr1} \end{bmatrix},\ M_{r1}^{ze} = M_{r1}^{zr1}. \quad [25]$$

In addition tractor-fixed velocities v_t^{xt} and v_t^{yt} are introduced with

$$\begin{bmatrix} \dot{r}_t^{xe} \\ \dot{r}_t^{ye} \end{bmatrix} = \mathbf{T}_{t,e} \begin{bmatrix} v_t^{xt} \\ v_t^{yt} \end{bmatrix}. \quad [26]$$

Now the still pending time derivative in Eq. [22] is performed in vehicle-fixed coordinates. Finally the matrix multiplications

$$\mathbf{T}_{t,e}^{-1} \begin{bmatrix} \frac{d}{dt}\left(\frac{\partial T}{\partial \dot{q}_1}\right) - \frac{\partial T}{\partial q_1} \\ \frac{d}{dt}\left(\frac{\partial T}{\partial \dot{q}_2}\right) - \frac{\partial T}{\partial q_2} \end{bmatrix} = \mathbf{T}_{t,e}^{-1} \begin{bmatrix} Q_1 \\ Q_2 \end{bmatrix} \quad [27]$$

and a multitude of purely trigonometric simplifications similar to those in the more concise example (Genta, 1997) results in the nonlinear differential equations

$$\begin{bmatrix} \dot{v}_t^{xt} \\ \dot{v}_t^{yt} \\ \ddot{\Psi}_t \\ \ddot{\delta}_{thr} \end{bmatrix} = \mathbf{f}\left(v_t^{xt}, v_t^{yt}, \dot{\Psi}_t, \dot{\delta}_{thr}, \delta_{thr}, \ddot{\delta}_{r1d}, \dot{\delta}_{r1d}, \delta_{r1d}, F_t^{xt}, F_t^{yt}, M_t^{zt}, F_{r1}^{xr1}, F_{r1}^{yr1}, M_{r1}^{zr1}\right) \quad [28]$$

The most important result is that Eq. [28] became independent of Ψ_t, which has been the last reference to earth-fixed coordinates making linearization impossible. Unfortunately stating function **f** in Eq. [28] completely as done for the more concise kinematic equations of motion Eq. [11–13] is of very little use, because the length of the resulting expression would account for approximately 1.5 pages in this paper. With the given steps however it is possible to repeat the derivation invoking a computer algebra system. The length of the result also illustrates the limitations of dynamic modeling using explicit differential equations in case of steering actuators between tractor and implement.

External forces and moments

In Eq. [28] external forces and moments are still stated in a general manner. Within this work external forces account for lateral disturbances modeling gravity on slopes as well as tire forces. Lateral disturbances are simply added to lateral forces $F_t^{yt}$and F_{r1}^{yr1} acting on the respective center of gravity. Tire forces are modeled assuming a linear side slip to tire force relation using simple cornering stiffness parameters. From Fig. 2 the lateral tire force at the tractor front wheel results in

$$\mathbf{F}_{tf} = C_{\alpha,tf}\alpha_{tf}\mathbf{e}_{ytf} \qquad [29]$$

with cornering stiffness $C_{\alpha,tf}$ and side slip angle

$$\alpha_{tf} = \delta_{tf} - \tan^{-1}\left(\frac{v_{tf}^{yt}}{v_{tf}^{xt}}\right) = \delta_{tf} - \tan^{-1}\left(\frac{v_t^{yt} + \dot{\Psi}_t l_{tf}}{v_t^{xt}}\right). \qquad [30]$$

Similar relations are used for tractor rear and implement tire forces, all together contributing to the forces and moments acting on tractor and implement c.g.

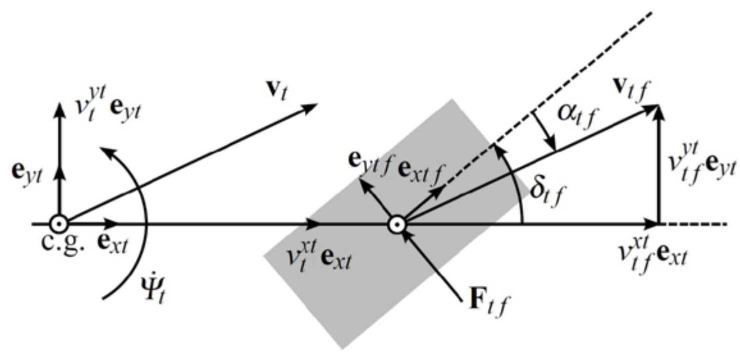

Fig. 2. Tractor front wheel showing velocity components v_{tf}^{xt} and v_{tf}^{yt} used for calculation of side slip angle α_{tf} and lateral tire force $\mathbf{F}_{tf}$.

Tracking Errors

Both kinematic and dynamic equations of motion so far hold independently of absolute vehicle position and heading. Those equations are based on linear and angular velocities and accelerations as well as hitch angle and drawbar steering angle. This is in agreement with what one would expect from underlying physics. Absolute vehicle position and heading could now be introduced by integrating linear and angular velocities. To allow for controller design and linearization however an expression of tractor and implement position in terms of deviations from a desired path is the better alternative. Tractor heading error e_{th} and lateral error e_{tl} shown in Fig. 1 are therefore defined using

$$\dot{e}_{th} = \dot{\Psi}_t - \dot{\Psi}_d, \qquad [31]$$

$$\dot{e}_{tl} = v_t^{xt}\sin(e_{th}) + \left(v_t^{yt} - l_{tr}\dot{\Psi}_t\right)\cos(e_{th}) \qquad [32]$$

with $\dot{\Psi}_d \equiv 0$ for straight line tracking. $\dot{\Psi}_t$ is given by Eq. [10] using the kinematic equations and found by integration of $\ddot{\Psi}_t$ using the dynamic equations. For straight line tracking the implement heading error e_{r1h} and lateral error e_{r1l} can be expressed using already existing systems states for both the kinematic and the dynamic equations of motion

$$e_{r1h} = e_{th} - \delta_{thr} - \delta_{r1d}, \qquad [33]$$

$$e_{r1l} = e_{tl} - \left(l_{r1r} + l_{r1f}\right)\sin(e_{th} - \delta_{thr} - \delta_{r1d}) - l_{r1d}\sin(e_{th} - \delta_{thr}) - l_{thr}\sin(e_{th}) . \qquad [34]$$

Steering Actuators

In order to complete the tractor and implement model steering actuator dynamics is introduced. This is done using a rather high-level description assuming underlying steering controllers enforcing a given steering angle command. Similar to (Karkee and Steward, 2010) a simple first order lag with time constant T_{tf} and input $\delta_{tf,d}$ is introduced for tractor front wheel steering. This is repeated for the implement wheel using the time constant T_{r1r} and input $\delta_{r1r,d}$, hence resulting in

$$\dot{\delta}_{tf} = \left(\delta_{tf,d} - \delta_{tf}\right)/T_{tf}\,, \qquad \dot{\delta}_{r1r} = \left(\delta_{r1r,d} - \delta_{r1r}\right)/T_{r1r}. \qquad [35]$$

From Eq. [12] and [28] can be seen that first and second order time derivative of the drawbar steering angle δ_{r1d} are inputs to the kinematic and the dynamic equations of motion. For the dynamic equations of motion in particular this is obviously due to $\ddot{\delta}_{r1d}$ being related to the moment required to steer the drawbar and to move the rigid bodies. Drawbar steering dynamics therefore is modeled using a second order delay with time constant T_{r1d}, damping ratio D_{r1d} and input $\delta_{r1d,d}$ resulting in

$$\ddot{\delta}_{r1d} = \left(\delta_{r1d,d} - 2D_{r1d}T_{r1d}\dot{\delta}_{r1d} - \delta_{r1d}\right)/T_{r1d}^2. \qquad [36]$$

PATH TRACKING CONTROL

Both the kinematic model Eq. [10–13] and the dynamic model Eq. [28–30] are used for controller design in this work in order to study the trade-off between controller performance and model parameterization effort. Each model is completed by tracking errors Eq. [31–34] and steering actuator dynamics Eq. [35] and [36]. Control theory for linear systems is used in both cases, therefore linear time invariant approximations of the kinematic and dynamic model are developed. This is done by assuming a constant forward velocity $v_t^{xt} \equiv v_{tc}^{xt}$ and performing a Taylor series expansion up to degree 1 about

$$\left[e_{tl}, e_{th}, v_t^{yt}, \dot{\Psi}_t, \delta_{thr}, \dot{\delta}_{thr}, \delta_{tf}, \delta_{r1d}, \dot{\delta}_{r1d}, \delta_{r1r}, \delta_{tf,d}, \delta_{r1d,d}, \delta_{r1r,d}\right]^T = \mathbf{0}. \qquad [37]$$

This results in two variants of the linear system

$$\dot{\boldsymbol{z}} = \mathbf{Az} + \mathbf{Bu}, \qquad \mathbf{y} = \mathbf{Cz}, \qquad [38]$$

$$\mathbf{u} = \left[\delta_{tf,d}, \delta_{r1d,d}, \delta_{r1r,d}\right]^T, \mathbf{y} = [e_{tl}, e_{th}, e_{r1l}, e_{r1h}]^T, \qquad [39]$$

with system states of the kinematic model's variant

$$\mathbf{z} = \left[e_{tl}, e_{th}, \delta_{thr}, \delta_{tf}, \delta_{r1d}, \dot{\delta}_{r1d}, \delta_{r1r}\right]^T, \qquad [40]$$

and the system states of the dynamic model's variant

$$\mathbf{z} = \left[e_{tl}, e_{th}, v_t^{yt}, \dot{\Psi}_t, \delta_{thr}, \dot{\delta}_{thr}, \delta_{tf}, \delta_{r1d}, \dot{\delta}_{r1d}, \delta_{r1r}\right]^T. \quad [41]$$

From a multitude of controllers applicable to system Eq. [37–41] a LQR state feedback controller with subsequent output feedback approximation originally proposed in (Werner et al., 2012) is chosen in this work. The main reason is that it allows for stating an identical design objective for both the kinematic and the dynamic model. In addition the same design objective can be chosen for arbitrary input combinations. Further this approach allows for purposive tuning based on weighting of tracking errors important for a particular task.

The first step is a standard LQR controller (Lunze, 2010) with state feedback

$$\mathbf{u} = -\mathbf{K}\mathbf{z}, \quad [42]$$

being designed to minimize the cost function

$$J = \int_0^\infty \left(\mathbf{y}^T(\mathrm{t})\mathbf{Q}\mathbf{y}(\mathrm{t}) + \mathbf{u}^T(\mathrm{t})\mathbf{R}\mathbf{u}(\mathrm{t})\right)dt. \quad [43]$$

The positive semi-definite and positive definite matrices $\mathbf{Q} = \left(q_{i,j}\right)$ and $\mathbf{R} = \left(r_{i,j}\right)$ are chosen to be diagonal with the remaining non-zero elements stating the actual weights of particular inputs and tracking errors.

In a second step a method taken from (Lunze, 2010) is used to approximate the state feedback Eq. [42] by output feedback

$$\mathbf{u} = -\mathbf{K}_y\mathbf{y}, \qquad \mathbf{K}_y = \mathbf{KVW}(\mathbf{CVW})^+. \quad [44]$$

$\mathbf{V}$ is the matrix of closed loop system eigenvectors resulting from state feedback, i.e. eigenvectors of $(\mathbf{A} - \mathbf{BK})$, and $(\bullet)^+$ denotes the pseudo inverse. With this method $\mathbf{K}_y$ is calculated to approximate the eigenvalues attained by state feedback $\mathbf{K}$. The diagonal weighting matrix $\mathbf{W}$ provides means to allow for better approximation of particular eigenvalues. In this work that is used to solely focus on the closed loop eigenvalue or the pair of closed loop eigenvalues with smallest absolute value, which normally (Föllinger, 1994) dominate the system's behavior.

SIMULATION RESULTS

Finally open loop system analysis and closed loop simulations are performed using both kinematic and dynamic model for controller design. Comparing the results supports choosing the appropriate model for a given task.

Parameters

Table 1 summarizes the parameters used in this section. Vehicle parameters originate from identifications performed by (Karkee and Steward, 2010) for a John Deere 7930 tractor and an unsteered towed Parker grain cart. Implement steering actuators have been added for the following simulations with their dynamics approximately matching tractor steering actuator dynamics identified by (Karkee and Steward, 2010).

Table 1. Simulation parameters with vehicle parameters based on identifications by (Karkee and Steward, 2010) for a John Deere 7930 tractor and a towed Parker 500 grain cart.

Tractor		Implement		Controller	
parameter	value	parameter	value	parameter	value
l_{tf}	1.7 m	l_{r1d}	1.62 m	$q_{1,1}$	100/(1 m)²
l_{tr}	1.2 m	l_{r1f}	2 m	$q_{2,2}$	1/(10 deg)²
l_{thr}	0.9 m	l_{r1r}	0.1 m	$q_{3,3}$	400/(1 m)²
m_t	9391 kg	m_{r1}	2127 kg	$q_{4,4}$	400/(10 deg)²
I_t	35709 kg m²	I_{r1}	6402 kg m²	$r_{1,1}$	10/(10 deg)²
$C_{\alpha,tf}$	220 kN/rad	$C_{\alpha,r1r}$	167 kN/rad	$r_{2,2}$	10/(10 deg)²
$C_{\alpha,tr}$	486 kN/rad	T_{r1d}	0.1 sec	$r_{3,3}$	10/(10 deg)²
T_{tf}	0.1 sec	D_{r1d}	0.7		
		T_{r1r}	0.1 sec		

The LQR controller is parameterized by choosing weights for the diagonal matrices **Q** and **R** in Eq. [43]. The weights in Table 1 are chosen to achieve proper implement positioning and alignment, i.e. implement lateral error e_{r1l} and implement heading error e_{r1h} are considered most important. Tractor lateral error e_{tl} is considered less important and tractor heading error e_{th} is neglected.

System Analysis

Fig. 3 depicts the open loop eigenvalues of both the kinematic and the dynamic variant of system Eq. [38–41]. Using the same steering actuator dynamics Eq. [35] and [36] results in two real eigenvalues at -10 and a conjugate complex pair at -7±7.141j for both variants. Tracking error differential equations originating from Eq. [31] and [32] cause two real eigenvalues at 0 in both linearized system variants. The kinematic system's remaining real eigenvalue results from hitch angle differential equation Eq. [11–13]. The remaining 4 eigenvalues of the dynamic model variant result from rigid body dynamics, two of those forming a conjugate complex pair at higher velocities as seen in Fig. 3(d). In general the eigenvalues close to the origin dominating the system's behavior are very similar for kinematic and dynamic model variant at velocities up to 4.5 m/sec. It is worth noting, that due to choosing the same parameters and performing linearization about zero implement steering angles the eigenvalues in Fig. 3 exactly match those given by (Karkee and Steward, 2010) despite having a chosen a fundamentally different approach to mechanics.

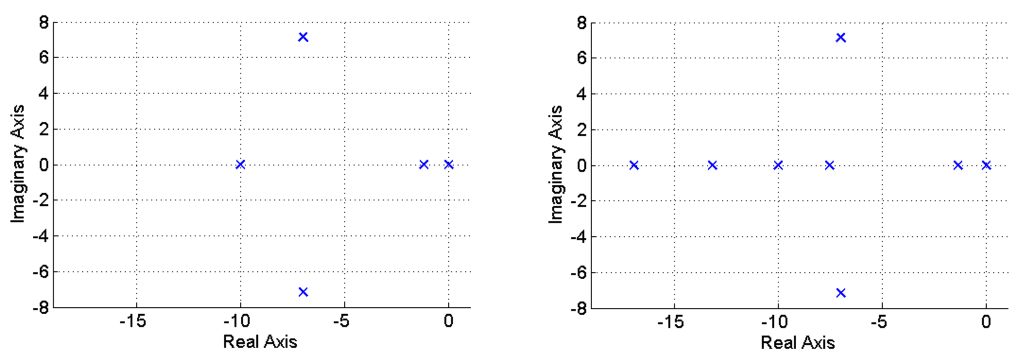

(a) kinematic (b) dynamic

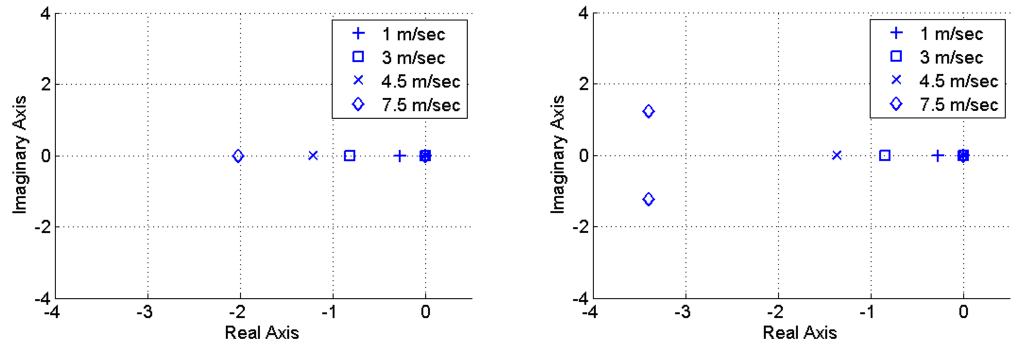

(c) kinematic (d) dynamic

Fig. 3. Eigenvalues of kinematic and dynamic open loop system at 4.5 m/sec tractor longitudinal velocity (a, b) and close-up view of eigenvalues near origin at several velocities (c, d).

Closed Loop Simulations

Finally this work presents closed loop simulation results using the non-linear dynamic plant model given by Eq. [28–36]. Both the kinematic and the dynamic model's linearized system descriptions Eq. [37–41] are used for controller design. Comparing full state feedback and output feedback approximation has already been subject to (Werner et. al, 2012) and this work is rather focused on comparing the results achievable using either a dynamic or a kinematic model for controller design. Of course using a kinematic model is desirable due to its simple parameterization based on geometric properties.

All simulations have been performed at 4.5 m/sec tractor longitudinal velocity and start with tractor and implement lateral errors of 1 m each. At 10 sec a lateral force step is applied to the tractor and steerable implement plant model accounting for disturbance forces resulting from gravity on a 30 deg slope.

Fig. 4 shows tracking errors and steering angles for controllers based on an either kinematic or dynamic model description. Tractor steering and various implement steering input combinations are used for those simulations. All controllers use the same weights in $\mathbf{Q}$ and $\mathbf{R}$, which are chosen to achieve precise implement positioning and orientation as stated in the parameters section. The most notable differences between kinematic and dynamic model based controllers are the tendency of overshooting and the larger steering angle amplitudes in case of a kinematic description. The impression of a more aggressively tuned controller resulting from a kinematic model description is supported by comparing the controllers' matrix 2- or ∞-norms being a rough indication for the controller gain. Using all steering inputs $\|\mathbf{K}_y\|_2$ is 1.7 for a dynamic and 2.0 for a kinematic model. $\|\mathbf{K}_y\|_\infty$ is 2.1 and 2.7 in those cases. Both kinematic and dynamic model based controller variants result in improved implement positioning by adding one steering actuator to the implement. Using both implement actuators is still advantageous for aligning the implement with the desired path.

In reality some dynamic model parameters are quite uncertain or even changing. This holds for tire cornering stiffness parameters for example, because they summarize tire as well as ground properties. Fig. 5 shows simulation results with cornering stiffness parameter values changed by ±50% compared to the values used for controller design stated in Table 1. Of course only controllers based on a dynamic model take cornering stiffness into account. The kinematic model based controllers neglect sliding properties right away. In both cases a decreased cornering stiffness increases overshooting and tendency of oscillations. Adapting model parameters or controller gain to changing cornering properties might therefore be a necessary remedy.

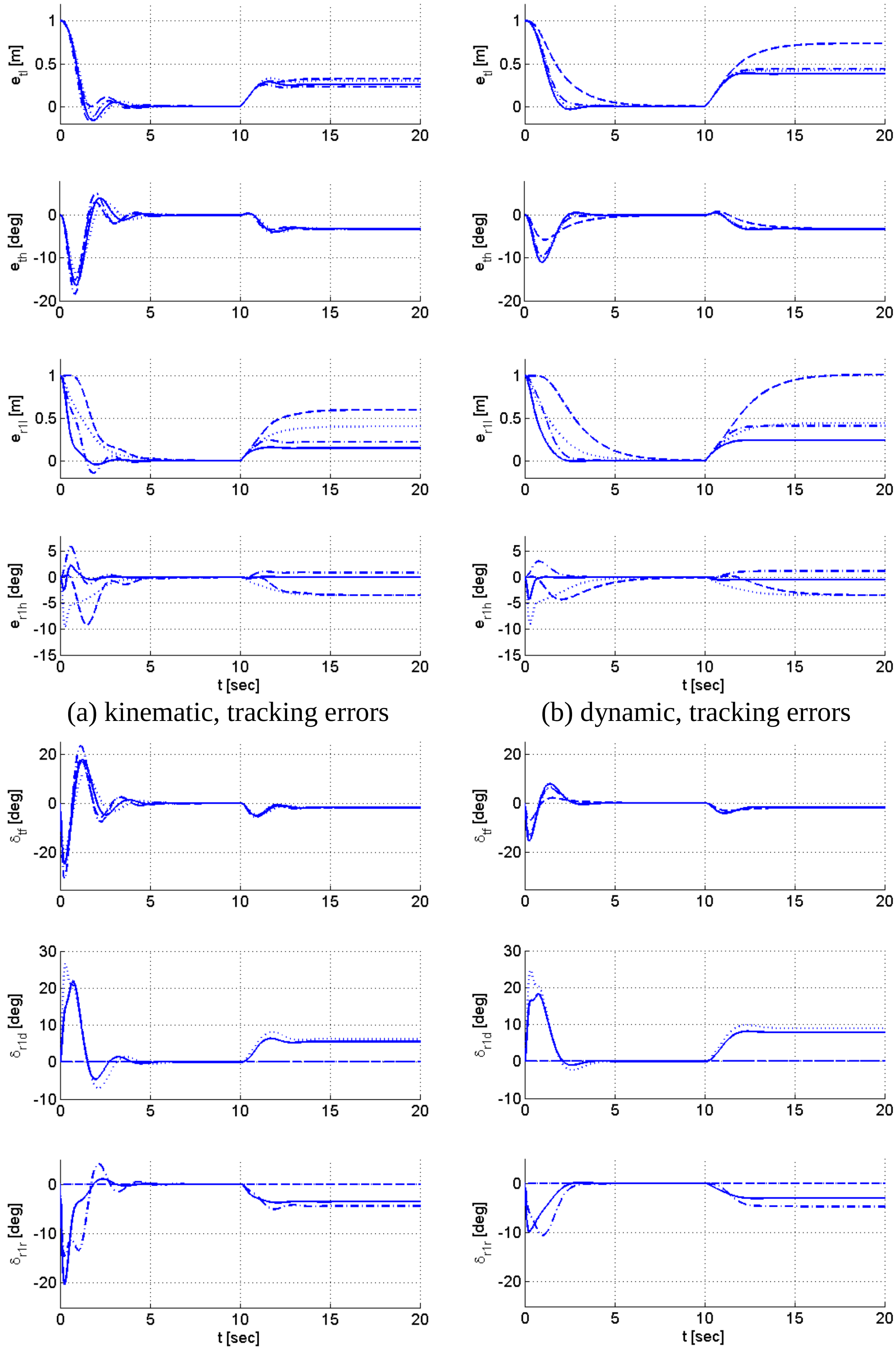

(a) kinematic, tracking errors (b) dynamic, tracking errors

(c) kinematic, steering angles (d) dynamic, steering angles

Fig. 4. Non-linear dynamic model simulation results with LQR output feedback controllers based on an either kinematic or dynamic model using tractor steering only (dashed), tractor and implement wheel steering (dash-dot), tractor and implement drawbar steering (dotted), and all inputs (solid).

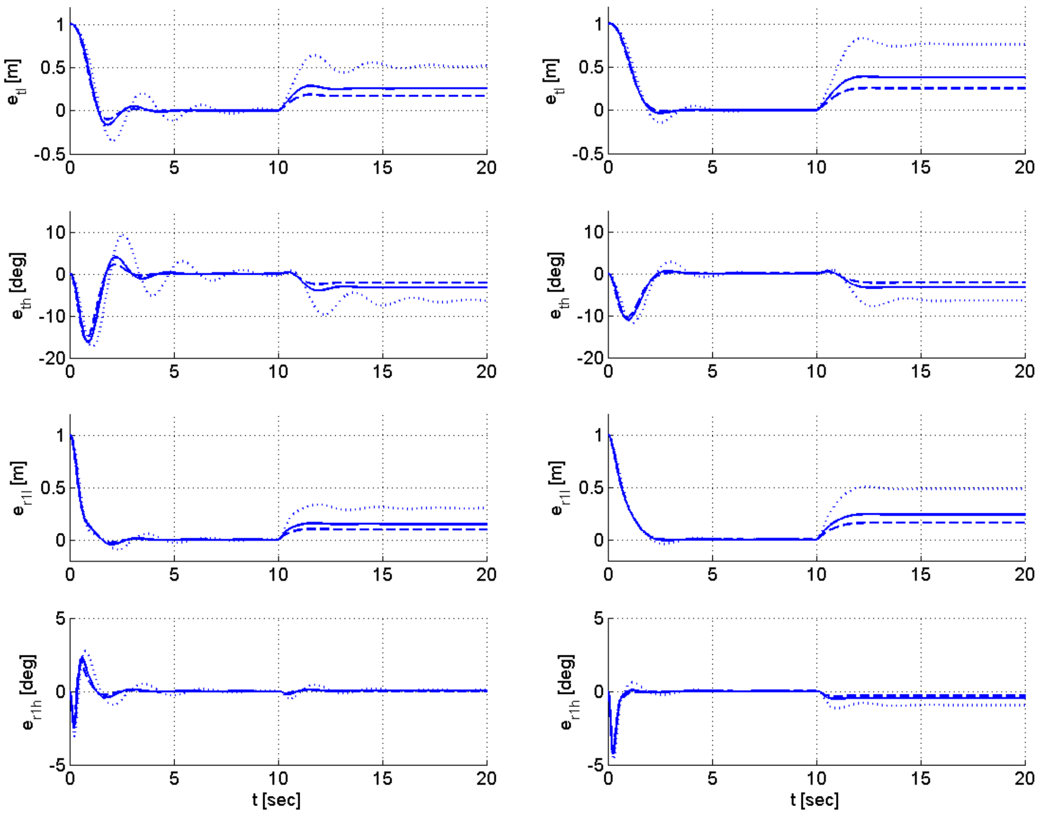

(a) kinematic, tracking errors (b) dynamic, tracking errors

Fig. 5. Non-linear dynamic model simulation results with LQR output feedback controllers based on an either kinematic or dynamic model using all steering inputs. The simulation cornering stiffness values are 50% higher (dashed), 50% lower (dotted), or equal (solid) to the values used for controller design.

CONCLUSION

Within this work systematic approaches to kinematic and dynamic modeling of a tractor towing an implement with steerable wheels and steerable drawbar have been presented. Dynamic modeling mainly relies on Lagrange's equations of motion and choosing proper generalized coordinates. As a consequence both approaches are very suitable for automated derivation of equations of motion using computer algebra systems, which actually has been used to produce the results of this paper. This automated derivation allows for simple model modifications and easy addition or replacement of actuators. In addition a flexible path tracking controller was presented, which can be used for both the kinematic and the dynamic model description. The controller is suitable for arbitrary steering actuator combinations, is based on intuitive tuning and only requires lateral and heading error for tractor and implement to be measured. System analysis and closed loop simulations have been performed using either a simple kinematic or a more detailed dynamic model for controller design. The simple kinematic model provided promising results up to at least 4.5 m/sec. For both the kinematic and the dynamic model based controller however adaption to a changing tire and soil properties might be necessary.

Acknowledgements
This research is supported by the European Regional Development Fund, the European Union, the state of Rheinland-Pfalz and John Deere.

Wachstum durch Innovation – EFRE

RheinlandPfalz

Diese Veröffentlichung wurde von der Europäischen Union aus dem Europäischen Fonds für regionale Entwicklung und vom Land Rheinland-Pfalz kofinanziert.

BIBLIOGRAPHY

Backman, J., et al., 2009. Parallel guidance system for tractor-trailer system with active joint. Eur. Conf. Precision Agric., 6–8 Jul., Wageningen: p. 615–622.

Bell, T., 1999. Precision robotic control of agricultural vehicles on realistic farm trajectories. Ph.D. diss., Stanford Univ., Stanford, CA.

Bevly, D.M., 2001. High speed, dead reckoning, and towed implement control for automatically steered farm tractors using GPS. Ph.D. diss., Stanford Univ., Stanford, CA.

Cariou, C., et. al., 2010. Path following of a vehicle-trailer system in presence of sliding: application to automatic guidance of a towed agricultural implement. IEEE/RSJ Int. Conf. Intelligent Robots and Systems, 18–22 Oct., Taipei, Taiwan: p. 4976–4981

Chen, C., Tomizuka, M., 1995. Dynamic modeling of articulated vehicles for automated highway systems. Proc. Am. Control Conf., Washington, DC: p. 653–657.

Föllinger, O., 1994. Regelungstechnik (In German). 8th ed. Hüthig, Heidelberg.

Genta, G., 1997. Motor vehicle dynamics. Series on advances in mathematics for applied sciences. Vol. 43. World Sci. Publ. Singapore.

Greenwood, D., 1988. Principles of dynamics. 2nd ed. Prentice Hall. Upper Saddle River, NJ.

Karkee, M., Steward, B.L., 2010. Study of the open and closed loop characteristics of a tractor and a single axle towed implement system. J. Terramechanics. 47:379–393.

Lunze, J., 2010. Regelungstechnik 2 (In German). 6th ed., Springer, Heidelberg.

Pota, H., et. al., 2007. Simulation of a tractor-implement model under the influence of lateral disturbances. 46th IEEE Conf. on Decision and Control, 12–14 Dec., New Orleans, LA: p. 596–601.

Siew, K.W., et. al., 2009. Simulation of an articulated tractor-implement-trailer model under the influence of lateral disturbances. IEEE/ASME Int. Conf. Advanced Intelligent Mechatronics, 14–17 Jul., Singapore: p. 951–956.

Werner, R., et. al., 2012. Dynamic modeling and path tracking control for a farm tractor towing an implement with steerable wheels and steerable drawbar. Commercial Vehicle Technol. Symp., 13–15 Mar., Kaiserslautern, Germany: p. 241–250.